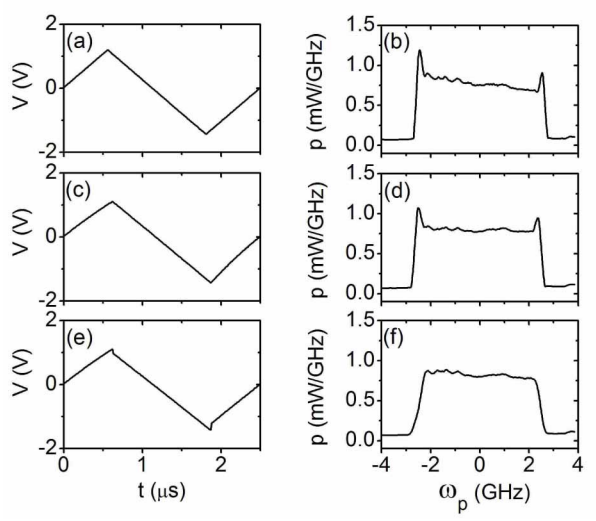

Fig. 2. Pump spectral distribution optimization procedure for the case of slow modulation. Modulation waveform $V(t)$ (left column) and measured pump spectrum profile $p(\omega_p)$ (right column) are shown for triangular modulation (upper row), with the addition of a small quadratic term (middle row), and for the optimum waveform (lower row). The DC injection current is 110 mA.

where $v_{\max} = 2.73$ V, and $a = -30.4\ \mu s^{-2}$. The parameters are optimized using the same error-minimizing iterative procedure. The RMSD for the optimal spectral profile is 0.069 mW/GHz (Fig. 2(f)), compared to 0.083 mW/GHz for Fig. 2(b) and 0.081 mW/GHz for Fig. 2(d).

We then measure the SBS gain profiles produced by the spectral broadened pump beam using the current modulation waveforms depicted in Fig. 1(g) (the "fast" modulation) and Fig. 2(e) (the "slow" modulation). The experiment setup is shown in Fig. 3. To independently measure the SBS gain profile, we use a weak unmodulated monochromatic signal beam (input power P_{s0}), and record the amplified signal beam power P_s at the photoreceiver as we slowly scan the frequency of the signal beam. The SBS power gain G is given by

$$G = \ln(P_s/P_{s0}). \tag{2}$$

The SBS power gain G is related to $g(\omega_s)$ by $G(\omega_s) = g(\omega_s)L_{eff}$, where $L_{eff} = (1-e^{-\alpha L})/\alpha =$ 1.64 km is the effective length of the fiber, L (= 2 km) is the physical length of the fiber and α (= 0.9 dB/km) is the attenuation coefficient of the fiber.

Figure 4(a) shows the measured SBS gain G profiles for the fast and slow modulation methods. As discussed previously, the SBS gain profile is the convolution of the pump spectrum with the intrinsic narrow Lorentzian lineshape. In our case where the pump spectrum bandwidth (5 GHz) is much larger than the narrow Lorentzain linewidth (∼52 MHz in HNLF), the resultant SBS gain profile is similar to the pump spectrum, as seen in Fig. 4(a). We see that the SBS gain profile is not as sharp on the edges using the fast noise-modulation waveform, which is due to the fluctuating temperature, as discussed above. On the other hand, the slow triangular-like waveform results in a deterministic value of the laser temperature at any moment. Therefore, the frequency of the laser is well-defined at the edge of the modulation waveform. However, this is not true for the fast noise modulation, where the temperature is affected by the previous history of the modulation and thus has wide fluctuations. However, as shown next, the reduced slope of the edges for the fast noise modulation does not substantially affect its slow light performance.

#136722 - $15.00 USD Received 18 Oct 2010; revised 19 Nov 2010; accepted 9 Dec 2010; published 5 Jan 2011

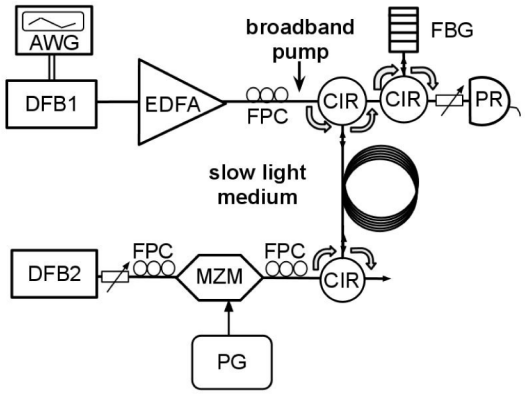

Fig. 3. Experiment setup. Spectrally broadened pump and signal beams counter-propagate in the 2-km-long slow light medium (HNLF, OFS Inc.), where they interact via the SBS process. The SBS frequency shift in HNLF is 9.62 GHz. A fiber Bragg grating (FBG, bandwidth 0.1 nm) is used to filter out the Rayleigh backscattering of the pump beam from the amplified and delayed signal pulse sequence before detection. AWG: arbitrary function generator (Tektronix AFG3251), DFB1: 1550-nm DFB laser diode (Sumitomo Electric, STL4416), EDFA: erbium doped fiber amplifier (IPG Photonics EAD 1K), DFB2: 1550-n DFB laser diode (Fitel FOL15DCWC), MZM: Mach-Zehnder Modulator, PG: electronic signal pattern generator, PR: 12 GHz photo-receiver (New Focus 1544b), FPC: fiber polarization controllers, CIR: optical circulator.

3. Slow-light performance

We next compare the delay performance of the fast and slow modulation methods. First, we use a continuous-wave signal beam ($P_{s0} = 48\ \mu$W) that is tuned to the SBS resonance to measure the line center SBS gain G at different pump powers. Again, G is obtained from Eq. (2). As shown in Fig. 4(b), both modulation formats result in identical linear growth of G with respect to the pump power P_p when it is low. As P_p increases, we see that the slow modulation method results in an early saturation in comparison to the case for the fast modulation waveform. Saturation takes place when the SBS gain G is large enough so that a great portion of the power in the

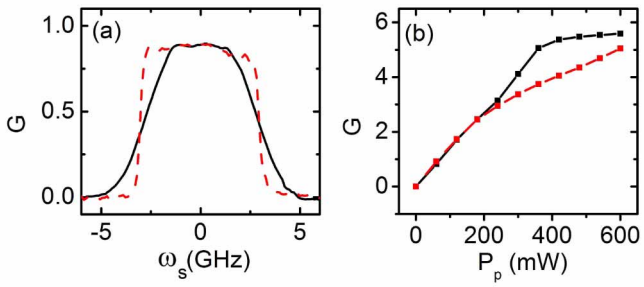

Fig. 4. (a) SBS gain profiles for fast (solid black line) and slow modulations (red dashed line) at $P_p = 70$ mW. (b) SBS gain saturation for fast and slow modulation methods. The black solid line shows the SBS gain G for the fast noise modulation, which grows linearly with pump power P_p until saturated. The red dashed line shows the SBS gain G for the slow modulation, which starts to saturate gradually at a much smaller P_p compared to the fast modulation method.

#136722 - $15.00 USD Received 18 Oct 2010; revised 19 Nov 2010; accepted 9 Dec 2010; published 5 Jan 2011

pump beam is transferred into the signal beam, and the exponential amplification of the signal beam cannot be sustained [20].

The early saturation in the slow modulation case is likely due to fluctuations in *G*. The fluctuation in *G* is related to the uneven frequency swept rate and the end effect. In the slow modulation method, the frequency of the pump beam is slowly swept. During the modulation period of 2.5 μs, a monochromatic signal beam is only intermittently amplified during the short time period when the pump-probe frequency difference is equal to the SBS frequency shift within the resonance linewidth. An estimate of the average interaction time period gives 52 MHz/5 GHz $\times$2.5 μs$=$ 26 ns. On this time scale, sweep rate fluctuations result from the short thermal constants of the DFB laser can significantly affect the length of the interaction time period and give rise to fluctuations in *G*. Moreover, since the SBS amplification process in the slow modulation method is intermittent, there is an end effect that induces more fluctuations in *G*. In our experiment specifically, the frequency of the pump beam as seen by the signal beam goes through a little less than 8 periods of modulation during the whole propagation time ($\sim$9.7 μs) through the 2-km-long HNLF. Since the number of modulation periods during the propagation time is not an exact integer, the signal beam can meet the resonant pump frequency for different times (7 or 8), depending on the relative time when we measure the waveform during the modulation period. As a result of both effects, the output signal beam measured at some particular time is amplified more than others and is more likely to saturate the gain. This behavior results in the gradual early saturation seen in Fig. 4(b).

In the fast modulation method, on the other hand, a monochromatic signal is constantly amplified by the frequency-matching component in the broadband pump beam as it travels through the fiber. Pump beam frequency chirping rate might still have uncontrolled jitter on a faster time scale beyond 400 MHz, but the SBS interaction cannot response to such fast processes. The output signal amplification results from the accumulated SBS interaction through the whole fiber. Therefore, *G* is uniform and stable in this case. The fluctuation in *G* for the slow modulation method is the source of the low-frequency fluctuations that degrades the fidelity of a data waveform.

The small number of scanning periods in the 2-km-long HNLF can be increased by substantially increasing the fiber length while keep the modulation rate slow. For this reason, in our experiment, a 20-km LEAF fiber is used for the slow light fidelity check in a long fiber. By doing that, we expect to reduce the fluctuations due to the end effect and provide more averaging along the fiber that can help reduce *G* fluctuation and stabilize the output signal. However, as shown next, a much longer fiber will increase noise from spontaneous Brillouin scattering [21, 22] and boost SBS *G* saturation, as a result of increased SBS gain coefficient. Also, dispersion of the fiber increases with length, which induces distortion to the signal pulse and degrade the performance. The possible fiber length increase is also limited by practical factors of cost and volume, and it is impossible to use this method to compensate for a modulation rate increase of 1000 as demonstrated in our experiment comparison between the fast and slow modulations.

To measure the delay and fidelity for a data sequence, we use our 5-GHz broadband SBS slow light system to delay a 2^{12} bit-long return-to-zero (RZ) binary data sequence. This data sequence contains all 2^8 8-bit-long sequences separated by 8-bits 0s serving as a buffer. In this arrangement, the pattern-dependent delay is averaged. The use of an RZ signal is more reliable in situations with pulse broadening effects, but takes twice as much bandwidth to achieve the same data rate compared to the non-RZ coding. A data rate of 2.5 Gb/s is used for the signal to match the SBS slow light bandwidth of 5 GHz (FWHM), where the width of a single pulse is equal to 200 ps. The data sequence is generated by a pattern generator (HP70004A) and encoded on the signal beam via the 10-GHz Mach-Zehnder Modulator (MZM). We use a weak

#136722 - $15.00 USD Received 18 Oct 2010; revised 19 Nov 2010; accepted 9 Dec 2010; published 5 Jan 2011

signal seed laser beam (power $P_{s0} = 12\ \mu$W) and restrict $P_p < 500$ mW to avoid SBS gain saturation in HNLF ($P_p < 300$ mW in LEAF). After propagating through the fiber, the delayed and amplified signal beam is detected by a 12-GHz photoreceiver and recorded on an 8-GHz digital sampling oscilloscope (Agilent DSO80804B). Slow light performance for the fast and slow modulation methods is evaluated by the well-known fidelity metrics of EO and SNR based on the eye-diagram of the output signal at various pump power levels.

We first measure the slow light pattern delay by generating the output eye diagram, which is essentially an overlap of the time domain output traces for a certain number of bit periods. The pattern delay is determined by comparing the position of the maximum eye-opening with and without the pump beam. Figure 5(a) shows the measured pattern delay for both the slow and fast pump modulation formats as a function of P_p. Since a weak signal beam is used in the measurement, the measured pattern delay goes linearly with P_p and no significant saturation is observed. Both modulation formats yield the same delay within the measurement error, which agrees well with the theoretical simulation delay time for a rectangular-like optimized gain profile [11] (blue dotted-dash line) and a super-Gaussian gain profile (cyan dash-double dot line). As shown in both experiment data and simulation, the reduced slope of the super-Gaussian gain profile in the fast modulation method does not significantly reduce the delay time. The reason for that could be traced in Fig. 5(b), where we observe the temporal profile of the output signal sequence. Shown in this figure are the averaged pulse profiles at $P_p = 350$ mW for the first "1" in the data sequence, which is an isolated pulse with many bits of "0"s before and after. We see that the delayed pulse shapes for both modulation methods are very close. Compared with the undelayed pulse shape, which is a super-Gaussian, we see that both fast and slow modulation SBS gain profiles re-shape the signal pulse into a Gaussian profile. This is because high temporal frequency components beyond the 5-GHz bandwidth are cut out. Nevertheless, the distortion is small. We can also see that the fast modulation method results in a more symmetric pulse profile, while the slow modulation method produces small ripples behind the main pulse whose profile is asymmetric. The better output pulse profile in the fast modulation method is a result of the smoother phase response for the super-Gaussian shaped gain profile. The asymmetric pulse shape for the slow modulation reduces the peak delay difference between the two methods, resulting in a very close delay performance observed in Fig. 5(a). Based on results shown in Figure 5(a) and (b), we see that both slow and fast modulations demonstrate similar delay and pulse distortion behaviors, allowing us to do the following fidelity performance comparison between these two methods.

Also shown in Fig. 5(a) is the pattern delay in the 20-km LEAF fiber using the slow modulation method. A steeper increase of delay time with P_p is observed as a result of increased Brillouin gain coefficient in the longer fiber. Pump power P_p is restricted within 300 mW to avoid SBS gain saturation.

We next study the signal fidelity of the slow light device. The slow light fidelity metrics are measured in terms of EO and SNR. The EO is measured by the maximum difference between the minimum value of high level and the maximum value of the low level in the eye diagram (shown in Fig. 6). The SNR at the eye-center is defined as the ratio of the EO with the quadratic mean of the standard deviations (noise) of the high and low levels.

Figure 5(c) shows the EO and Fig. 5(d) shows the SNR as functions of P_p. Note that as we change P_p, the power of the signal beams goes through 3-4 orders of magnitude, which is beyond the dynamic range of most photoreceiver. In our experiment, an detection attenuation is set to avoid detector saturation at $P_p = 500$ mW in HNLF ($P_p = 300$ mW in LEAF). As the output signal beam is amplified with increasing P_p, the signal fidelity first increases as the signal overtakes the detector dark noise, then decreases when the SBS gain approaches saturation at high pump power, where amplified spontaneous Brillouin scattering begins to dominate [21].

#136722 - $15.00 USD Received 18 Oct 2010; revised 19 Nov 2010; accepted 9 Dec 2010; published 5 Jan 2011

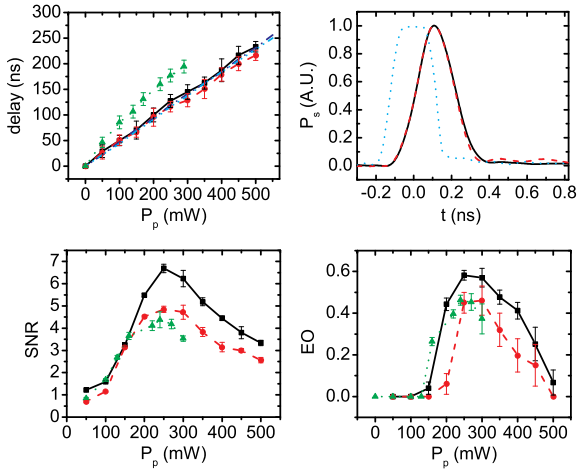

Fig. 5. Slow light performance for fast (solid black line) and slow (dashed red line) modulation waveforms in HNLF, and slow modulation waveform in LEAF (dotted green line). (a) Slow light delay as a function of P_p. The theoretically predicted delay for a rectangular-like optimized gain profile (blue dash-dot line) and for a super-Gaussian gain profile (cyan dash-double dot line) in the HNLF fiber are also shown. SBS gain saturation is avoided using a signal data sequence with a small peak optical power $P_{s0} = 12$ μW; (b) Averaged output signal profiles at $P_p = 350$ mW for the first single pulse in the data sequence, together with the undelayed pulse profile at $P_p = 0$ mW (blue dotted line) in HNLF. Both fast and slow modulation methods result in very similar pulse profile modification without significant broadening. The amplitude of the pulses is normalized as a percentage of the peak pulse height; Fidelity metrics are shown in (c) EO and (d) SNR as functions of P_p, demonstrating better performance for the fast modulation.

Comparing the slow light performance for the fast and slow modulation methods in the HNLF fiber, we see that while both modulation methods result in similar trends for signal quality at different pump power levels, the fast noise-modulation method results in better data fidelity over all pump power levels. In particular, Fig. 6 shows an example of the output eye diagrams for both modulation methods at $P_p = 350$ mW, where 50% more EO is obtained for the fast modulation method. A fractional delay (ratio of the delay with the width of a single pulse) of 0.81 with a SNR of 5.2 is achieved at $P_p = 350$ mW for the fast modulation method. Compared to the slow modulation method, the fast modulation method increases the EO by 50% and SNR by 36%, demonstrating significant enhancement of data fidelity with the same delay.

The SNR and EO in the 20-km LEAF fiber using the slow modulation method are also shown in Fig. 5 (c) and (d). We see that the trend of the fidelity curves as a function of P_p in LEAF has the similar shape, but the P_p level corresponding to the high fidelity peak is lower due to a larger Brillouin gain coefficient. In the small P_p (< 200 mW) region, the LEAF fiber has demonstrated fidelity improvement compared to the HNLF fiber using the slow modulation method. In the high P_p (> 200 mW) region, as a result of larger spontaneous Brillouin amplification noise, the fidelity of the signal drops down in the LEAF fiber. Overall, the slow light performance in the much longer LEAF fiber demonstrate improvement in the small P_p region, but a much better performance is obtained using the fast modulation method in HNLF at all P_p levels.

#136722 - $15.00 USD Received 18 Oct 2010; revised 19 Nov 2010; accepted 9 Dec 2010; published 5 Jan 2011

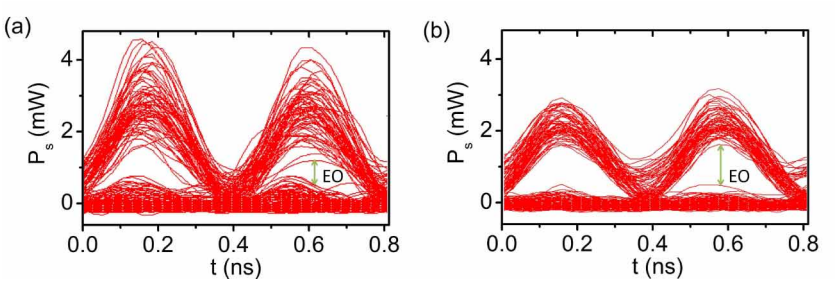

Fig. 6. Eye diagrams of delayed and amplified data sequences for (a) slow and (b) fast modulation waveforms at $P_p = 350$ mW in HNLF. The arrows in the figure show the EO for each case.

4. Conclusion

We have shown that the signal fidelity is significantly improved in a broadband SBS slow light system using noise current modulation of the pump beam spectrum. The SBS gain profile is tailored by controlling the distribution of the noise-modulation waveform. We obtain an optimal flat-topped gain profile using an asymmetric bi-peak-distributed noise-modulation waveform. Using this broadband SBS slow light technique, we significantly improve the signal fidelity compared to previous low-frequency slow synthesized waveform modulation methods. Pattern delays up to 1 pulse width is obtained with high fidelity for RZ data rate of 2.5 Gb/s.

Acknowledgements

We gratefully acknowledges the financial support of the DARPA Defense Sciences Office Slow Light project.

#136722 - $15.00 USD Received 18 Oct 2010; revised 19 Nov 2010; accepted 9 Dec 2010; published 5 Jan 2011